Polytechnic University of Turin
Master's Degree Program in Aerospace Engineering
Academic Year 2022/2023

Designing a cantilevered support using Fused Deposition Modeling (FDM) manufacturing technology

Federico Cocuzza Santuccio

Contents

List of Figures

Chapter 1

Designing a cantilevered support using Fused Deposition Modeling (FDM) manufacturing technology

1.1 Instructions on the support

The assigned task involves designing a cantilevered support to be attached to a square-sectioned aluminum beam with dimensions of 4x4 cm, using three constraints: one on the central face of the beam and two on the right and left lateral faces. To ensure the stability of the support, M6 bolts with an anchoring hole diameter of 6.5 mm are planned to be used. The loads will be applied at a distance of 100 mm from the front face of the beam. It is specified that the reference material for the production of the support is Onyx.

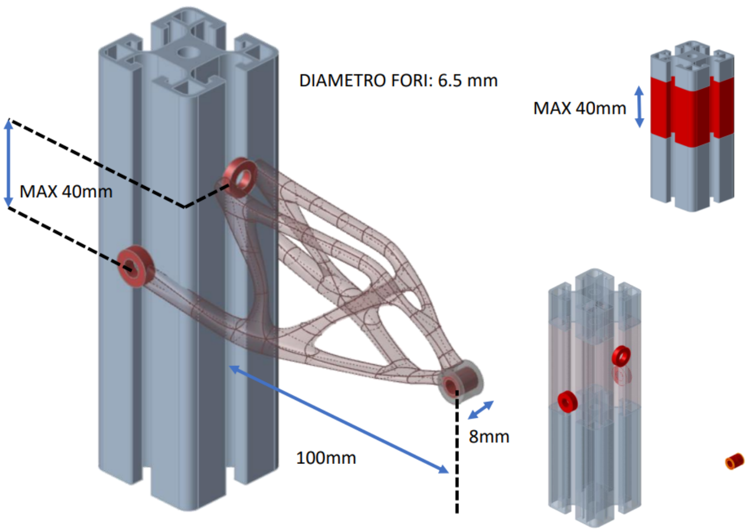

Figure 1.1

1.2 Objectives

The support must be able to meet the following constraints:

- Support two independent loads, one in the Z direction and the other in the X direction, both with a value of 5.02 N.
- Displacement along the Z-axis should not exceed $1mm$.
- Displacement along the X-axis should not exceed $2mm$.
- The safety factor values should be greater than 2.

Three different solutions have been designed to address these requirements.

1.3 Analysis procedure

Regarding the analysis method employed, two different loading conditions have been defined.

1. **Loading Condition 1**
   - Support 1 and 2 completely fixed (free rotation around the X-axis)
   - Support 3 completely fixed
   - Force 1 (Z-axis): 5.02 N
   - Displacement constraint 1: 1 mm (Z-axis)
2. **Loading Condition 2**
   - Support 1 and 2 completely fixed (free rotation around the X-axis)
   - Support 3 completely fixed
   - Force 1 (X-axis): 5.02 N
   - Displacement constraint 1: 2 mm (X-axis)

1.4 Support design

The three design alternatives have been developed with the shared objective of reducing the component's mass. Specifically, the second solution was conceived to minimize the volume and the quantity of supports required during the printing phase. To achieve this, in the initial configuration, the anchor points were positioned at a closer distance compared to what was adopted in the first design.

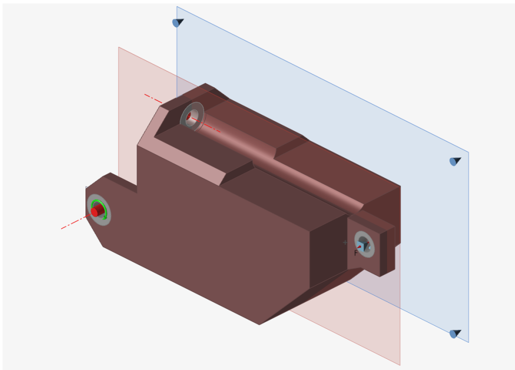

Figure 1.2: Initial Volume Design 1

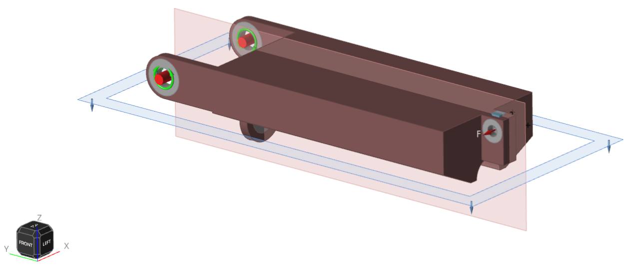

Figure 1.3: Initial Volume Design 2

1.5 Setting up optimizations

Regarding the optimizations, in addition to the previously mentioned loading conditions, we set a symmetry check on the Y-Z axis to enhance the final result. Furthermore, to minimize the use of support structures during 3D printing, we oriented the component horizontally, establishing a direction of extraction along the Z-axis. This choice allowed us to reduce material usage and the time required for production. It should be noted that all models were made using Onyx as the reference material. Below is a representative image of the analysis configuration.

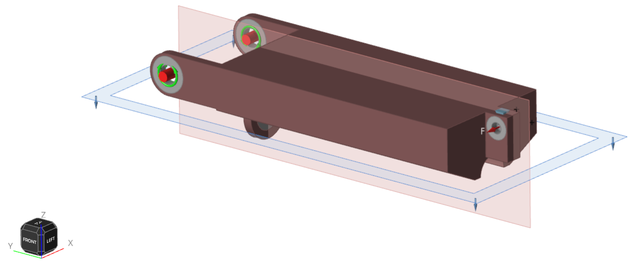

Figure 1.4: Analysis Configuration

1.6 Design solutions

1.6.1 Design 1

Regarding the first design, a distance of 40 mm was adopted between the axes of the anchor points, positioning the front one at a higher level than the other two. This solution was achieved through a topological optimization aimed at reducing the component's mass by 80% compared to the original model and improving its stiffness. The achieved result is shown in Figure ??.

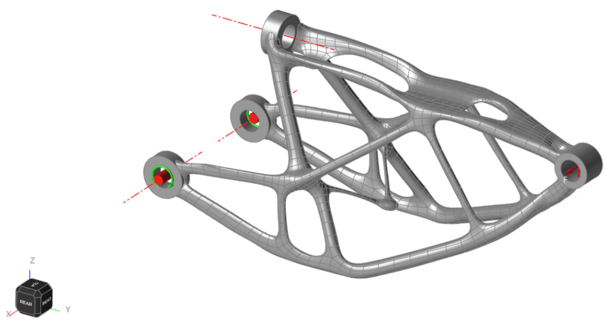

Figure 1.5

Static analysis

Below are the outcomes of the static analysis applied to the first design.

1. **Loading Condition 1 (Force 5.02 N along Z-axis)**

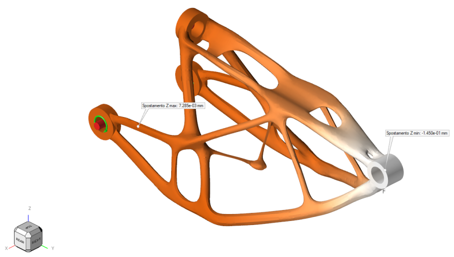

(a) Maximum Displacement: 0.15 mm

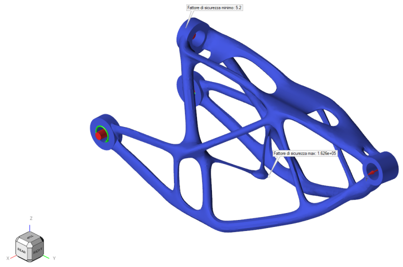

(b) Minimum Safety Factor: 5.2

Figure 1.6

2. **Loading Condition 2 (Force 5.02 N along X-axis)**

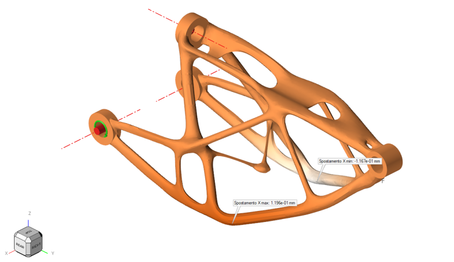

(a) Maximum Displacement: 0.12 mm

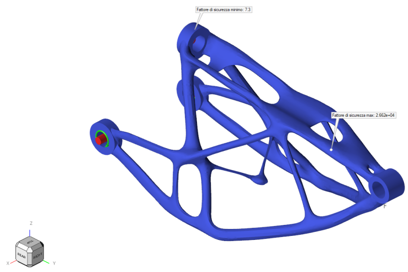

(b) Minimum Safety Factor : 7.3

Figure 1.7

Buckling analysis

Deformation analyses of the structure were conducted for both loading conditions, considering the first 10 natural modes. The goal was to assess whether the applied loads could pose a criticality to the structure. For each mode of deformation considered, the Buckling Load Factor (BLF) consistently remained much greater than 1, indicating that the structure is capable of withstanding the applied loads.

1.6.2 Design 2

For this particular design, we chose a hook distance of 15 mm, aiming to reduce the moment of inertia of the structure and the overall volume of the component. Additionally, unlike the first design, we positioned the front hook lower than the other two. Once again, the final component was generated through topological optimization, aimed at minimizing the mass while maintaining a safety factor greater than 2. Subsequently, we further optimized the structure using the *PolyNURBS shape optimization* command provided by the Inspire software. The result obtained is presented below:

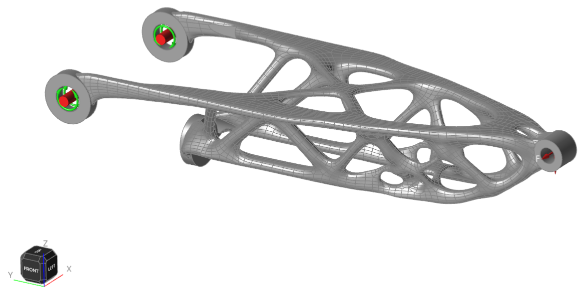

Figure 1.8: Analysis Configuration

Static analysis

Below are the outcomes of the static analysis applied to the second design.

1. **Loading Condition 1 (Force 5.02 N along Z-axis)**

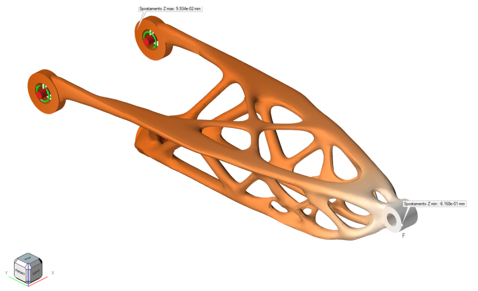

(a) Maximum Displacement: 0.6 mm

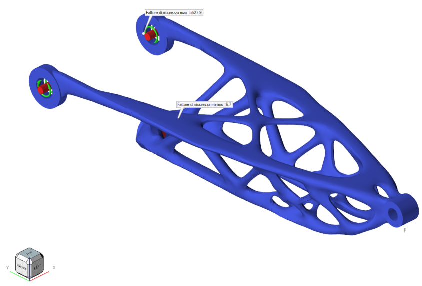

(b) Minimum Safety Factor: 6.7

Figure 1.9

2. **Loading Condition 2 (Force 5.02 N along X-axis)**

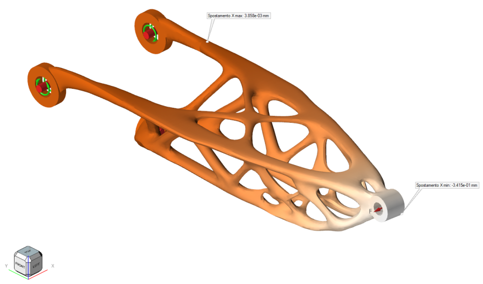

(a) Maximum Displacement: 0.3 mm

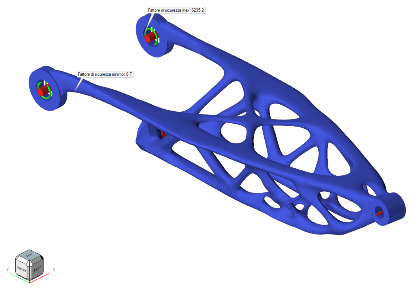

(b) Minimum Safety Factor: 8.7

Figure 1.10

Buckling analysis

In this case as well, for both loading conditions, a test was conducted regarding deformations considering the first 10 natural modes of the structure, and it resulted in BLF consistently much greater than 1. Once again, the structure is sufficiently capable of withstanding the applied loads.

1.6.3 Design 3

For this solution, we began with the starting model from solution 2 and applied a topological optimization to reduce the mass by 60%. Subsequently, we conducted a further lattice-type optimization, setting the filling parameter to 100%, reducing the mass by an additional 20%. The default values of target length, minimum diameter, and maximum diameter of the lattice provided by the *Inspire* software were kept unchanged. The final result is as follows:

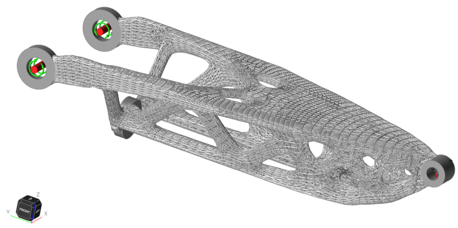

Figure 1.11: Analysis Configuration

Static analysis

Below are the outcomes of the static analysis applied to the third design.

1. **Loading Condition 1 (Force 5.02 N along Z-axis)**

(a) Maximum Displacement: 1 *mm*

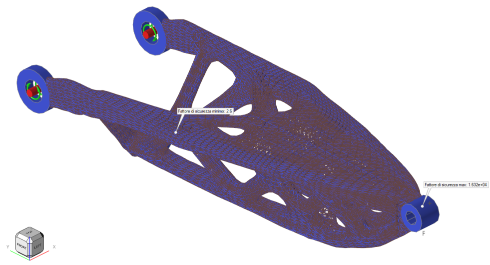

(b) Minimum Safety Factor: 2.6

Figure 1.12

2. **Loading Condition 2 (Force 5.02 N along X-axis)**

(a) Maximum Displacement: 0.6 *mm*

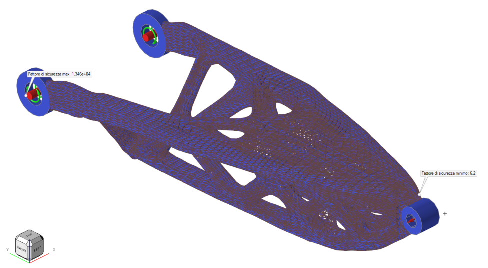

(b) Minimum Safety Factor: 6.2

Figure 1.13

Buckling analysis

In this case as well, for both loading conditions, a test was conducted regarding deformations considering the first 10 natural modes of the structure, and it resulted in BLF consistently greater than 1. Once again, the structure is capable of withstanding the applied loads.

1.7 Comparison of the three solutions

	Design 1	**Design 2**	**Design 3**
Maximum Displacement F_z	0.15 mm	0.6 mm	1 mm
Minimum Safety Factor F_z	5.2	6.7	2.6
Maximum Displacement F_x	0.12 mm	0.3 mm	0.6 mm
Minimum Safety Factor F_x	7.3	8.7	6.2

Table 1.1: Summary table of the data

In addition to the data derived from their respective analyses, printing simulations were conducted using the slicing software "*eiger.io*" and the Onyx material, in order to obtain realistic estimates of print time, final model weight, and material cost. The values of these parameters for each of the three designs considered are reported in Table 1.2.

	Design 1	**Design 2**	**Design 3**
Volume (cm^3)	46	16.14	23
Mass (g)	12.9	11.02	9.47
Layer Thickness (mm)	0.2	0.2	0.2
Number of walls	2	2	2
Printing Time (ore:min)	6+:00	3:05	9+:00
Costs (USD)	11.13	3.83	8.42

Table 1.2: Summary table of the 3D printing simulation data

In conclusion, from the data presented, it is evident that the second design exhibits superior characteristics in terms of time, costs, safety factor, and criticality. Particularly, in the selection of this design, the duration of the printing time played a decisive role, with a maximum limit set at 3 hours.